Black Sea Journal of Engineering and Science

doi: 10.34248/bsengineering.1919861

Open Access Journal
e-ISSN: 2619 – 8991

Research Article
Volume 9 - Issue 4: 1556-1567 / July 2026

A ROBUST METHOD FOR THE NUMERICAL SOLUTION OF THE ADVECTION-DIFFUSION EQUATION USING THE GALERKIN METHOD BASED ON HERMITE B-SPLINE FUNCTIONS

Halil BEYAZIT[1]*, Sibel ÖZER[1], Yusuf UÇAR[1]

[1]*Inönü University, Faculty of Science, Department of Mathematics, 44280, Malatya, Türkiye*

Abstract: The goal of this research is to find an approximate solution to the one-dimensional linear advection-diffusion equation using the cubic Hermite B-Spline Galerkin finite element method, a new numerical method developed by selecting cubic Hermite B-spline functions as the basis functions. After discretizing the advection-diffusion equation in the temporal direction using the Crank-Nicolson formula, the spatial discretization of the semi-discrete scheme was performed using cubic Hermite B-spline functions. The effectiveness and accuracy of the proposed method were tested using the four most well-known model problems in the literature. The obtained numerical results were compared with those of other studies in the literature and presented in tabular form. Additionally, to observe the agreement of the approximate solutions with the analytical solution of the model problems, the graphs of the analytical and the approximate solutions were plotted together, and the graphs of the absolute error were plotted.

Keywords: Galerkin method, Advection-diffusion equation, Hermite B-spline function, Finite element method, Legendre polynomials

***Corresponding author:** Inönü University, Faculty of Science, Department of Mathematics, 44280, Malatya, Türkiye
E mail: halilbeyazt@gmail.com (H. BEYAZIT)
Halil BEYAZIT https://orcid.org/0000-0002-0854-2301
Sibel ÖZER https://orcid.org/0000-0003-4956-4002
Yusuf UÇAR https://orcid.org/0000-0003-1469-5002

Received: March 31, 2026
Accepted: May 17, 2026
Published: July 15, 2026

Cite as: Beyazıt, H., Özer, S., & Uçar, Y. (2026). A robust method for the numerical solution of the advection-diffusion equation using the galerkin method based on hermite b-spline functions. *Black Sea Journal of Engineering and Science*, 9(4), 1556-1567.

1. Introduction

This paper deals with the one-dimensional Advection-Diffusion (AD) equations 1-3 defined as;

$$u_t + \alpha u_x - \mu u_{xx} = 0, x \in [a,b], t \geq 0, \quad (1)$$

with initial condition,

$$u(x,0) = f(x), x \in [a,b] \quad (2)$$

and boundary conditions,

$$u(a,t) = \gamma_1(t), u(b,t) = \gamma_2(t), t \geq 0 \quad (3)$$

where $\gamma_1(t), \gamma_2(t)$ and $f(x)$ are known functions, $\alpha > 0$ is flow velocity constant and $\mu > 0$ is the diffusion constant. It is clear that the AD equation given by equation 1 reduces to the one-dimensional heat equation for $\alpha = 0$. The AD equation given by equation 1 is a partial differential equation that describes the transport and diffusion of physical quantities such as mass, heat and energy (Dehghan, 2004; Mittal and Jain, 2012). Whereas the term "advection" in the equation 1 refers to the movement of molecules within fluids, the term "diffusion" describes the random movement of particles from regions of high density to regions of low density. This means that $u(x,t)$ represents the concentration at position x and time t. In addition, the AD equation is used to mathematically explain many phenomena related to heat transfer, fluid mechanics, chemistry, biology, environmental sciences, and other disciplines. Several of these include heat transfer in a drainage film Isenberg and Gutfinger (1973) water transfer in soils Parlange (1980), the spread of underground water pollution Guvanasen and Volker (1983), long-range transport of pollutants in the atmosphere Zlatev et al. (1984), the propagation of pollutants in rivers and streams Chatwin and Allen (1985), the movement of drugs within body tissues (Chapman et al., 2008; Naghipoor et al., 2018) and the voluminous concentration of a pollutant Goh et al. (2012).

Although the analytical solution to the AD equation, which models certain physical phenomena in nature, may be available for specific conditions, they can sometimes be computationally expensive. Moreover, physical phenomena may be more complicated than expected. For this reason, scientists have developed approximate solutions to the AD equation under various boundary and initial conditions. The following methods have been proposed to find approximate solutions to the AD equation: weighted finite difference scheme Dehghan (2004), finite difference scheme Salkuyeh (2006), unconditionally stable finite difference scheme Karahan (2007), high-order compact scheme Mohebbi and Dehghan (2010), Taylor-Galerkin finite element method Kadalbajoo and Arora (2010), Taylor-Galerkin method Dağ et al. (2011), cubic B-spline collocation method

Mittal and Jain (2012), exponential B -spline collocation method Mohammadi (2013), cubic Hermite collocation method for linear and nonlinear AD equation Mittal et al. (2013), differential quadrature approach using quartic and quintic B-spline methods Korkmaz and Dağ (2016), matrix equation-based strategies Palitta and Simoncini (2016), a fourth-order numerical method using cubic B-spline functions Mittal and Rohila (2020), UMIST scheme as a position discretization for the finite difference method Ünal (2022), a high-order B-spline Galerkin method Iqbal et al. (2023), an open near-optimal quantum algorithm Novikau and Joseph (2025).

In this paper, we have used a cubic Hermite Galerkin finite element method to find numerical solutions of the AD equation given by equation 1 with the initial and boundary conditions given by equation 2 and equation 3, respectively. In Section 2, the cubic Hermite Galerkin finite element method is presented. In Section 3, numerical examples are used to test the present method, and obtained numerical results are given in tables and graphics. In Section 4, a brief conclusion is given.

2. Materials and Methods

Suppose $a = x_1 < x_2 < \cdots < x_N < x_{N+1} = b$ is a uniform partition of the interval $[a,b]$ and $h = x_{k+1} - x_k, k = 1(1)N$. For $k = 1(1)N$, at the x_k knots points, the cubic Hermite B-spline functions H_{2k-1} and H_{2k} are defined on the interval $[x_{k-1}, x_{k+1}]$ as follows (Prenter, 1989; Ganaie and Kukreja, 2014):

$$H_{2k-1} = \begin{cases} 2\left(\frac{x-x_{k-1}}{h}\right)^3 - 3\left(\frac{x-x_{k-1}}{h}\right)^2 + 1, x \in [x_{k-1}, x_k] \\ -2\left(\frac{x-x_k}{h}\right)^3 + 3\left(\frac{x-x_k}{h}\right)^2 + 1, x \in [x_k, x_{k+1}] \\ 0, \quad \text{otherwise} \end{cases} \tag{4a}$$

and

$$H_{2k} = \begin{cases} 2\left(\frac{x-x_{k-1}}{h}\right)^3 - 3\left(\frac{x-x_{k-1}}{h}\right)^2 + 1, x \in [x_{k-1}, x_k] \\ -2\left(\frac{x-x_k}{h}\right)^3 + 3\left(\frac{x-x_k}{h}\right)^2 + 1, x \in [x_k, x_{k+1}] \\ 0, \quad \text{otherwise.} \end{cases} \tag{4b}$$

There are $2N + 2$ the cubic Hermite B-spline functions in the interval $[a,b]$. Now, we apply the local coordinate transformation defined as $h\xi = x - x_j$ to express the cubic Hermite B-spline functions given by equations 4a and 4b in terms of the local coordinate parameter ξ. In this case, a typical finite interval $[x_j, x_{j+1}]$ is mapped to the interval [0,1], the cubic Hermite B-spline functions in terms of local parameter ξ over the element [0,1] and their derivatives are as follows:

$$\left.\begin{array}{ll} \widehat{H}_1(\xi) = (1+2\xi)(1-\xi)^2, & \widehat{H}_1'(\xi) = 6(\xi^2 - \xi), \\ \widehat{H}_2(\xi) = h\xi(1-\xi)^2, & \widehat{H}_2'(\xi) = h(1 - 4\xi + 3\xi^2), \\ \widehat{H}_3(\xi) = 3\xi^2 - 2\xi^3, & \widehat{H}_3'(\xi) = 6(\xi - \xi^2), \\ \widehat{H}_4(\xi) = h(\xi^3 - \xi^2), & \widehat{H}_4'(\xi) = h(3\xi^2 - 2\xi), \end{array}\right\} \tag{5a}$$

$$\left.\begin{array}{l} \widehat{H}_1''(\xi) = 6(2\xi - 1), \\ \widehat{H}_2''(\xi) = h(6\xi - 4), \\ \widehat{H}_3''(\xi) = 6(1 - 2\xi), \\ \widehat{H}_4''(\xi) = h(6\xi - 2). \end{array}\right\} \tag{5b}$$

Let $U(x,t)$ be the approximate solution corresponding to the analytical solution $u(x,t)$ of the AD equation. Thus, the approximate value $U(x_j, t_n)$ at the nodal point (x_j, t_n) is denoted by U_j^n. Since the cubic Hermite B-spline functions have been chosen as the approximation functions, the approximate solution $U(x,t)$ is written as;

$$u(x,t) \approx U(x,t) = \sum_{j=1}^{2(N+1)} H_j(x) a_j(t) \tag{6}$$

where $a_j(t)$ are the time-dependent parameters to be determined. The non-zero cubic Hermite B-spline functions on $e_k = [x_k, x_{k+1}]$ for $k = 1(1)N$ are H_{2k-1}, H_{2k}, H_{2k+1} and H_{2k+2}. This enables fast computation and low memory usage by taking advantage of the benefits of sparse matrices. Then, the approximate solution given by equation 6 is denoted by;

$$U(x,t) = \sum_{j=2k-1}^{2k+2} H_j(x) a_j(t) \tag{7}$$

for the interval $[x_k, x_{k+1}]$. When the indices of the approximate solution given by equation 7 are adjusted,

$$U(x,t) = \sum_{j=1}^{4} H_{(j+2k-2)}(x) a_{j+2k-2}(t) \tag{8}$$

is obtained. The first and second derivatives of approximate solution given by;

$$U_x(x,t) = \sum_{j=1}^{4} H_{x(j+2k-2)}(x) a_{j+2k-2}(t), \tag{9a}$$

$$U_{xx}(x,t) = \sum_{j=1}^{4} H_{xx(j+2k-2)}(x) a_{j+2k-2}(t) \tag{9b}$$

respectively. Furthermore, when the local coordinate transformation $h\xi = x - x_j$ is applied to the derivatives U_x and U_{xx} given by equations 9a and 9b, $hd\xi = dx \Rightarrow d\xi/dx = 1/h$ since $U_x = U_\xi/h$ and $U_{xx} = U_{\xi\xi}/h^2$ the approximate solution and its derivatives can be expressed in terms of local parameter as;

$$U(x,t) = \sum_{j=1}^{4} \widehat{H}_j(\xi) a_{j+2k-2}(t), \tag{10a}$$

$$U_x(x,t) = \frac{1}{h}\sum_{j=1}^{4} \widehat{H}_j'(\xi) a_{j+2k-2}(t), \tag{10b}$$

$$U_{xx}(x,t) = \frac{1}{h^2}\sum_{j=1}^{4} \widehat{H}_j''(\xi) a_{j+2k-2}(t). \tag{10c}$$

We will now examine the time discretization of the AD equation given by equation 1. Assume that $0 = t_0 < t_2 < \cdots < t_{M-1} < t_M = T$ is a uniform partition of the interval $[0,T]$ and $\Delta t = t_{n+1} - t_n, n = 0(1)M$. When the AD equation is discretized using the Crank-Nicolson method as;

$$\frac{u^{n+1} - u^n}{\Delta t} + \alpha \frac{u_x^{n+1} + u_x^n}{2} - \mu \frac{u_{xx}^{n+1} - u_{xx}^n}{2} = 0 \tag{11}$$

a semi-discrete scheme is obtained (Başhan et al., 2018; Başhan et al., 2020). If we rearrange equation 11,

$$u^{n+1} + r_1 u_x^{n+1} - r_2 u_{xx}^{n+1} = u^n - r_1 u_x^n + r_2 u_{xx}^n \tag{12}$$

is obtained where $r_1 = \alpha\Delta t/2, r_2 = \mu\Delta t/2$.

To obtain the weighted residual form, which is one of the steps in the Galerkin method, equation 12 is multiplied by the weight function $w(x)$ and integrated over the interval $[a,b]$,

$$\int_a^b w u^{n+1} dx + r_1 \int_a^b w u_x^{n+1} dx - r_2 \int_a^b w u_{xx}^{n+1} dx$$
$$= \int_a^b w u^n dx - r_1 \int_a^b w u_x^n dx + r_2 \int_a^b w u_{xx}^n dx. \tag{13}$$

When partial integration is applied to the $\int_a^b w u_{xx} dx$

term in equation 13, the weak form as;

$$\int_a^b wu^{n+1}dx + r_1\int_a^b wu_x^{n+1}dx + r_2\int_a^b w_x u_x^{n+1}dx$$
$$-r_2 wu_x^{n+1}|_a^b = \int_a^b wu^n dx - r_1\int_a^b wu_x^n dx$$
$$+r_2\int_a^b w_x u_x^n dx - r_2 wu_x^n|_a^b \tag{14}$$

is found. Since equation 14 is true on $[a,b]$ interval, it also is true for the subinterval $[x_k, x_{k+1}] \subseteq [a,b]$. So, the weak form is written as following;

$$\int_{x_k}^{x_{k+1}} wu^{n+1}dx + r_1\int_{x_k}^{x_{k+1}} wu_x^{n+1}dx + r_2\int_{x_k}^{x_{k+1}} w_x u_x^{n+1}dx$$
$$-r_2 wu_x^{n+1}|_{x_k}^{x_{k+1}} = \int_{x_k}^{x_{k+1}} wu^n dx - r_1\int_{x_k}^{x_{k+1}} wu_x^n dx$$
$$+r_2\int_{x_k}^{x_{k+1}} w_x u_x^n dx - r_2 wu_x^n|_{x_k}^{x_{k+1}}. \tag{15}$$

After substituting the approximate solution and its derivatives given by equations 8, 9a and 9b, for the terms u, u_x, and u_{xx} in equation 15 , and substituting the cubic Hermite B-spline functions given by equations 4a and 4b for the weight function, the resulting equation is obtained by applying the local coordinate transformation $h\xi = x - x_k$ local coordinate transformation is applied to the resulting equation, the interval $[x_k, x_{k+1}]$ is mapped to the interval [0,1]. In addition, if the local variable representations given by equations 10a, 10b and 10c are substituted for the approximate solutions U, U_x, and U_{xx} and the local parameters given by equations 5a and 5b are substituted for the cubic Hermite B-spline functions in the equation obtained via local transformation, in this case, if we consider for $i = 1(1)4$ $dH_i/dx = (d\widehat{H}_i/d\xi)(d\xi/dx) \Rightarrow H_x = \widehat{H}_i'/h$ the equation,

$$\int_0^1 \widehat{H}_i \sum_{j=1}^4 \widehat{H}_j a_{j+2k-2}^{n+1} d\xi + \frac{r_1}{h}\int_0^1 \widehat{H}_i \sum_{j=1}^4 \widehat{H}_j' a_{j+2k-2}^{n+1} d\xi$$
$$+\frac{r_2}{h^2}\int_0^1 \widehat{H}_i' \sum_{j=1}^4 \widehat{H}_j' a_{j+2k-2}^{n+1} d\xi - \frac{r_2}{h}\left(\widehat{H}_i \sum_{j=1}^4 \widehat{H}_j' a_{j+2k-2}^{n+1}\right)_0^1$$
$$= \int_0^1 \widehat{H}_i \sum_{j=1}^4 \widehat{H}_{ji} a_{j+2k-2}^{n} d\xi + \frac{r_1}{h}\int_0^1 \widehat{H}_i \sum_{j=1}^4 \widehat{H}_j' a_{j+2k-2}^{n} d\xi$$
$$+\frac{r_2}{h^2}\int_0^1 \widehat{H}_i' \sum_{j=1}^4 \widehat{H}_j' a_{j+2k-2}^{n} d\xi - \frac{r_2}{h}\left(\widehat{H}_i \sum_{j=1}^4 \widehat{H}_j' a_{j+2k-2}^{n}\right)_0^1 \tag{16}$$

is obtained. Equation 16 can be written in a clearer manner by putting it in parentheses as;

$$\sum_{j=1}^4 \left(\int_0^1 \widehat{H}_i\widehat{H}_j d\xi + \frac{r_1}{h}\int_0^1 \widehat{H}_i\widehat{H}_j' d\xi\right) a_{j+2k-2}^{n+1}$$
$$+\sum_{j=1}^4 \left(\frac{r_2}{h^2}\int_0^1 \widehat{H}_i'\widehat{H}_j' d\xi - \frac{r_2}{h}\widehat{H}_i\widehat{H}_j'\Big|_0^1\right) a_{j+2k-2}^{n+1}$$
$$= \sum_{j=1}^4 \left(\int_0^1 \widehat{H}_i\widehat{H}_j d\xi + \frac{r_1}{h}\int_0^1 \widehat{H}_i\widehat{H}_j' d\xi\right) a_{j+2k-2}^{n}$$
$$+\sum_{j=1}^4 \left(\frac{r_2}{h^2}\int_0^1 \widehat{H}_i'\widehat{H}_j' d\xi - \frac{r_2}{h}\widehat{H}_i\widehat{H}_j'\Big|_0^1\right) a_{j+2k-2}^{n} \tag{17}$$

In equation 17 the integrals are defined as $\hat{A}_{ij} = \int_0^1 \widehat{H}_i\widehat{H}_j d\xi$, $\hat{B}_{ij} = \int_0^1 \widehat{H}_i\widehat{H}_j' d\xi$, $\hat{C}_{ij} = \int_0^1 \widehat{H}_i'\widehat{H}_j' d\xi$, $\widehat{D}_{ij} = \widehat{H}_i\widehat{H}_j'|_0^1$ where k is the number of elements and j = 1, 2, 3, 4,

$$\left(\hat{A}^e + \frac{r_1}{h}\hat{B}^e + \frac{r_2}{h^2}\hat{C}^e - \frac{r_2}{h}\widehat{D}^e\right) a_{j+2k-2}^{n+1}$$
$$= \left(\hat{A}^e - \frac{r_1}{h}\hat{B}^e - \frac{r_2}{h^2}\hat{C}^e + \frac{r_2}{h}\widehat{D}^e\right) a_{j+2k-2}^{n} \tag{18}$$

the numerical scheme is obtained. Here, the matrices $\hat{A}^e$, $\hat{B}^e$, $\hat{C}^e$ and $\widehat{D}^e$ are 4×4 square matrices. The matrices obtained by calculating the integrals are shown below:

$$\hat{A}^e = \begin{bmatrix} \frac{13}{35} & \frac{11h}{210} & \frac{9}{70} & \frac{-13h}{420} \\ \frac{11h}{210} & \frac{h^2}{105} & \frac{13h}{420} & \frac{-h^2}{140} \\ \frac{9}{70} & \frac{13h}{420} & \frac{13}{35} & \frac{-11h}{210} \\ \frac{-13h}{420} & \frac{-h^2}{140} & \frac{-11h}{210} & \frac{h^2}{105} \end{bmatrix}, \hat{B}^e = \begin{bmatrix} \frac{-1}{2} & \frac{h}{10} & \frac{1}{2} & \frac{-h}{10} \\ \frac{-h}{10} & 0 & \frac{h}{10} & \frac{-h^2}{60} \\ \frac{-1}{2} & \frac{-h}{10} & \frac{1}{2} & \frac{h}{10} \\ \frac{h}{10} & \frac{h^2}{60} & \frac{-h}{10} & 0 \end{bmatrix},$$

$$\hat{C}^e = \begin{bmatrix} \frac{6}{5} & \frac{h}{10} & \frac{-6}{5} & \frac{h}{10} \\ \frac{h}{10} & \frac{2h^2}{15} & \frac{-h}{10} & \frac{-h^2}{30} \\ \frac{-6}{5} & \frac{-h}{10} & \frac{6}{5} & \frac{h}{10} \\ \frac{h}{10} & \frac{-h^2}{30} & \frac{-h}{10} & \frac{2h^2}{15} \end{bmatrix}, \widehat{D}^e = \begin{bmatrix} 0 & -h & 0 & 0 \\ 0 & 0 & 0 & 0 \\ 0 & 0 & 0 & h \\ 0 & 0 & 0 & 0 \end{bmatrix}.$$

In the global system created by combining the element matrices $\hat{A}^e$, $\hat{B}^e$, $\hat{C}^e$ and $\widehat{D}^e$, the general rows of the matrices A, B, C and D

$$A = \frac{1}{420}\begin{pmatrix} 54 & 13h & 312 & 0 & 54 & -13h \\ -13h & -3h^2 & 0 & 8h^2 & 13h & -3h^2 \end{pmatrix},$$
$$B = \frac{1}{60}\begin{pmatrix} -30 & -6h & 0 & 12h & 120 & -6h \\ 6h & h^2 & -12h & 0 & 6h & -h^2 \end{pmatrix},$$
$$C = \frac{1}{30}\begin{pmatrix} -36 & -3h & 72 & 6h & -36 & 3h \\ 3h & -h^2 & 0 & 8h^2 & -3h & -h^2 \end{pmatrix},$$
$$D = \begin{pmatrix} 0 & 0 & 0 & 0 & 0 & 0 \end{pmatrix}$$

and the numerical scheme in the global system is created in the following form:

$$\left(A + \frac{r_1}{h}B + \frac{r_2}{h^2}C - \frac{r_2}{h}D\right) a_{j+2k-2}^{n+1}$$
$$= \left(\mathrm{A} - \frac{r_1}{h}B - \frac{r_2}{h^2}C + \frac{r_2}{h}D\right) a_{j+2k-2}^{n} \tag{19}$$

where equation 19 is a system of inhomogeneous algebraic equations consisting of 2N+2 equations and 2N+2 unknowns.

Applying the boundary conditions to equation 19, the left-hand boundary condition is $U(a,t) = \gamma_1(t)$, and from equation 9,

$$H_1(a)a_1(t) + H_2(a)a_2(t) + H_3(a)a_3(t) + H_4(a)a_4(t)$$
$$= \gamma_1(t) \tag{20}$$

is written. Since $H_2(a) = H_3(a) = H_4(a) = 0$, and $H_1(a) = 1$ substituting these values into the equation 20 yields $a_1(t) = \gamma_1(t)$ for all t. Similarly, from the right-hand boundary condition $U(b,t) = \gamma_2(t)$, and from equation 9,

$$H_{2\mathrm{N}-1}(a)a_{2\mathrm{N}-1}(t) + H_{2\mathrm{N}}(a)a_{2\mathrm{N}}(t) + H_{2\mathrm{N}+1}(a)a_{2\mathrm{N}+1}(t)$$
$$+H_{2\mathrm{N}+2}(a)a_{2\mathrm{N}+2}(t) = \gamma_1(t) \tag{21}$$

is written. Since $H_{2N-1}(b) = H_{2N}(b) = H_{2N+2}(b) = 0$ and $H_{2N+1}(b) = 1$ substituting these values into the equation 21 yields $a_{2N+1}(t) = \gamma_2(t)$ for all t. If the known values $a_1(t)$ and $a_{2N+1}(t)$ are substituted into the system of equation 19, the number of unknowns will be $2N$. To obtain a solvable system of equations, the number of equations must equal the number of unknowns. Consequently, if the first and $(2N-1)$th equations are removed from the system of equation 19 the new system of equations, which is the application of the boundary conditions, is expressed in matrices form as;

$$KX^{n+1} = LX^n + R, n = 0(1)M-1 \tag{22}$$

where for $i, j = 1(1)2N$

$K = [k_{ij}] = \left[A + \frac{r_1}{h}B + \frac{r_2}{h^2}C - \frac{r_2}{h}D\right]_{2N\times 2N}$,

$L = [l_{ij}] = \left[A + \frac{r_1}{h}B + \frac{r_2}{h^2}C - \frac{r_2}{h}D\right]_{2N\times 2N}$,

$$R = \begin{bmatrix} l_{11}\gamma_1^n - k_{11}\gamma_1^{n+11} \\ l_{21}\gamma_1^n - k_{21}\gamma_1^n \\ 0 \\ \vdots \\ 0 \\ l_{2N+1,2N+1}\gamma_2^n - k_{2N+1,2N+1}\gamma_2^{n+1} \\ l_{2N+2,2N+1}\gamma_2^n - k_{2N+2,2N+1}\gamma_2^{n+1} \end{bmatrix}_{2N\times 1}$$

and

$X = [a_2 \quad a_3 \quad \cdots \quad a_{2N-1} \quad a_{2N} \quad a_{2N+2}]^T$.

In this case, an initial value X^0 is required to proceed with iterative solutions for the system of equation 22. For this to occur, the number of equations must equal the number of unknowns. Therefore, considering the initial condition given by equation 2, $N+1$ equations were obtained from the equality $U(x_k,0) = f(x_k)$. This is insufficient to determine the initial values. Although there are $2N+2$ unknowns, there are only $N+1$ equations. Additional equations are therefore required. For this reason, points known as inner points were used in the initial condition given by equation 2.

Namely, given the points $x_1 = a$, $x_{N+1} = b$ and the roots of the quadratic Legendre polynomial $\mp 1/\sqrt{3} \in [-1,1]$, the equivalent of these points in a typical subinterval $[x_k, x_{k+1}]$ for $i = 1,2$ and $k = 1(1)N$ is;

$$\eta_{ki} = \frac{x_{k+1}+x_k}{2} + (-1)^i \frac{h}{2\sqrt{3}} \tag{23}$$

in the form. If the local coordinate transformation $h\xi = x - x_k$ is applied to roots given by equation 23, values $\xi_1 = \left(1 - 1/\sqrt{3}\right)/2$ and $\xi_2 = \left(1 + 1/\sqrt{3}\right)/2$, the roots of the shifted quadratic Legendre polynomial in the interval [0,1], is obtained and the relations $\eta_{k1} = h\xi_1 + x_k, \eta_{k2} = h\xi_2 + x_k$ exist. If the inner points given by equation 23 are substituted into equation 2, where $i = 1,2$ and k is the number of elements, $U(\eta_{ki},0) = f(\eta_{ki})$ is obtained. Besides, we could write,

$$\widehat{H}_{1i}a_{2k-1}^0 + \widehat{H}_{2i}a_{2k}^0 + \widehat{H}_{3i}a_{2k+1}^0 + \widehat{H}_{4i}a_{2k+2}^0 = f(\eta_{ki}) \tag{24}$$

due to $\widehat{H}_1(\xi_i) = H_{2k-1}(\eta_{ki})$, $\widehat{H}_2(\xi_i) = H_{2k}(\eta_{ki})$, $\widehat{H}_3(\xi_i) = H_{2k+1}(\eta_{ki})$, $\widehat{H}_4(\xi_i) = H_{2k+2}(\eta_{ki})$. If the predetermined values $a_1^0 = \gamma_1^0$ and $a_{2N+1}^0 = \gamma_2^0$ are substituted into the equation 24 and the resulting equation is rearranged matrices form such that

$$EX^0 = F \tag{25}$$

where

$$E = \begin{bmatrix} \widehat{H}_{21} & \widehat{H}_{31} & \widehat{H}_{41} & 0 & 0 & 0 & 0 & 0 \\ \widehat{H}_{22} & \widehat{H}_{32} & \widehat{H}_{42} & 0 & 0 & 0 & 0 & 0 \\ \widehat{H}_{11} & \widehat{H}_{21} & \widehat{H}_{31} & \widehat{H}_{41} & 0 & 0 & 0 & 0 \\ \widehat{H}_{12} & \widehat{H}_{22} & \widehat{H}_{32} & \widehat{H}_{42} & 0 & 0 & 0 & 0 \\ & & & \cdots & & & & \\ 0 & 0 & 0 & 0 & \widehat{H}_{11} & \widehat{H}_{21} & \widehat{H}_{31} & \widehat{H}_{41} \\ 0 & 0 & 0 & 0 & \widehat{H}_{12} & \widehat{H}_{22} & \widehat{H}_{32} & \widehat{H}_{42} \\ 0 & 0 & 0 & 0 & 0 & \widehat{H}_{11} & \widehat{H}_{21} & \widehat{H}_{41} \\ 0 & 0 & 0 & 0 & 0 & \widehat{H}_{12} & \widehat{H}_{22} & \widehat{H}_{42} \end{bmatrix}_{2N\times 2N}$$

and

$$F = \begin{bmatrix} f(\eta_{11}) - \widehat{H}_{11}\gamma_1^0 \\ f(\eta_{12}) - \widehat{H}_{12}\gamma_1^0 \\ f(\eta_{21}) \\ f(\eta_{22}) \\ \vdots \\ f(\eta_{N-1,1}) \\ f(\eta_{N-1,2}) \\ f(\eta_{N1}) - \widehat{H}_{31}\gamma_2^0 \\ f(\eta_{N2}) - \widehat{H}_{32}\gamma_2^0 \end{bmatrix}_{2N\times 1}.$$

In this way, the values of X^0 are calculated from equation 25 and the consecutive calculations are performed.

3. Results

In this section, the proposed method in Section 2 is applied to five model problems. The error norms of the obtained numerical results were calculated using the following formulas (equations 26a and 26b),

$$L_\infty = \|u - U\|_\infty = \max_{1\le k\le N} |u_k^n - U_k^n|, \tag{26a}$$

$$L_2 = \|u - U\|_2 = \left(h\sum_{k=1}^{N} |u_k^n - U_k^n|^2\right)^{1/2}. \tag{26b}$$

The Courant number C_r, the diffusion number S and the Peclet number P_e which are dimensionless parameters used in the analysis of numerical calculations of the AD equation, are calculated as follows:

$$C_r = \alpha\frac{\Delta t}{h}, S = \mu\frac{\Delta t}{h^2}, P_e = \frac{C_r}{S} = \frac{\alpha}{\mu}h \tag{27}$$

The advection term dominates for high values of the Peclet number, whereas the diffusion term dominates for low values of the Peclet number Mohammadi (2013).The obtained numerical results are given in the tables and graphics for various parameters. Throughout this paper, the initial and boundary conditions given by equation 2 and equation 3 were determined using the analytical solution of the equation. All numerical calculations were obtained using MatlabR2022b program on 16G RAM, 2.70 GHz computer.

Problem 1: We consider the AD equation with following the analytical solution given by for $x \in [0,L], t \in [0,T]$,

$$U(x,t) = \frac{\tau_0}{\tau}\exp\left(-\frac{(x-x_0-\alpha t)^2}{2\tau^2}\right) \tag{28a}$$

where $\tau^2 = \tau_0^2 + 2\mu t$ Rizwan (1997).

In equation 28a, we take $L = 1, \tau_0 = 0.025$, $x_0 = -0.5$, $\alpha = 1$ and $\mu = 0.01$ as given in Dehghan (2004) and then the exact solution is obtained as,

$$U(x,t) = \frac{0.025}{\sqrt{0.000625+0.02t}}\exp\left(-\frac{(x+0.5-t)^2}{0.00125+0.04t}\right). \tag{28b}$$

The comparison of the absolute errors at times $t = 1.0, 2.0, 3.0$ for Problem 1 with parameters $h = 0.01, \Delta t = 0.001$ are presented in Table 1. It is seen from table that the absolute errors of the present method were less than errors in the other studies. Subsequently, $h = \Delta t = 0.01$ spatial and temporal step sizes were selected and the comparison table of the approximate and exact solutions at time $t = 1.0$ is given in Table 2.

Table 1. A comparison of the absolute error at various x and $t = 1.0, 2.0, 3.0$ of Problem 1: $h = 0.01, \Delta t = 0.001$

x	Present	Nazir et al. (2016)	Mohammadi (2013)	Mittal and Jain (2012)	Present	Nazir et al. (2016)	Mohammadi (2013)	Mittal and Jain (2012)	Present	Nazir et al. (2016)
		t=1.0				t=2.0				t=3.0
0.1	1.20e-07	2.28e-06	1.04e-06	1.06e-06	1.05e-15	1.00e-13	1.00e-13	1.01e-13	5.70e-27	1.09e-23
0.2	3.39e-07	1.46e-06	5.01e-06	5.02e-06	4.72e-14	3.60e-12	3.61e-12	3.65e-12	1.17e-25	7.47e-22
0.3	6.21e-07	9.22e-06	1.82e-05	1.82e-05	1.20e-12	7.38e-11	7.49e-11	7.56e-11	6.49e-25	3.20e-20
0.4	2.68e-06	3.11e-06	1.01e-05	1.08e-05	2.07e-11	1.01e-09	1.02e-09	1.06e-09	1.84e-22	1.01e-18
0.5	5.40e-07	3.91e-06	4.57e-05	4.63e-05	2.55e-10	9.79e-09	1.00e-08	1.04e-08	9.38e-21	2.43e-17
0.6	3.91e-06	2.49e-05	4.04e-06	4.17e-06	2.27e-09	6.57e-08	7.24e-08	7.27e-08	3.07e-19	4.42e-16
0.7	2.39e-06	1.67e-05	3.72e-05	3.78e-05	1.47e-08	2.99e-07	3.45e-07	3.53e-07	7.23e-18	5.78e-15
0.8	1.09e-06	1.89e-05	7.05e-06	7.10e-06	6.79e-08	8.35e-06	1.13e-06	1.14e-06	1.22e-16	4.33e-14
0.9	1.32e-06	1.99e-05	8.88e-06	8.98e-06	2.17e-07	8.96e-06	2.09e-06	2.12e-06	1.22e-15	1.43e-13

Table 2. A comparison of approximate solutions obtained at time $t = 1.0$ for Problem 1: $h = \Delta t = 0.01$

x	Exact	Present	Kadalbajoo and Arora (2010)	Mittal and Jain (2012)
0.1	0.0035992	0.0035870	0.0035860	0.0035861
0.2	0.0196423	0.0196085	0.0196139	0.0196139
0.3	0.0660099	0.0660733	0.0660910	0.0660911
0.4	0.1366028	0.1368714	0.1368574	0.1368574
0.5	0.1740777	0.1741278	0.1740807	0.1740807
0.6	0.1366028	0.1362103	0.1362195	0.1362195
0.7	0.0660099	0.0657757	0.0658153	0.0658154
0.8	0.0196423	0.0197517	0.0197571	0.0197572
0.9	0.0035992	0.0037290	0.0037190	0.0037190

It can be seen that the approximate solution by the present method comply very well with the results of exact and other studies. Taking $P_e = 0.5, 1.0, 2.0, 4.0$ the exact and numerical solutions are also depicted at $t = 0.6, 0.8, 1.0, 1.2$ for $h = 0.01$, $\Delta t = 0.001$ in Figure 1. As shown from Figure 1, the waves generated by an increase in the Peclet numbers have greater amplitude and more completed waveforms.

Problem 2: The analytical solution of this problem is given by (Cecchi and Pirozzi, 2005; Mohebbi and Dehghan, 2010) as,

$$U(x,t) = e^{-t}\sin(x - \mu t), x \in [0,2], t \in [0,1]. \quad (29)$$

The numerical solution by presented method of Problem 2 was calculated by selecting $h = 1/64$, $\Delta t = 0.05h$ at $t = 1.0$, and the comparison table of absolute errors is presented in Table 3 for $P_e = 1000, 10000, 20000$ and $\mu = 1$. From Table 3, it is clearly shown that presented method achieves good results even at high Peclet numbers and is superior to other studies. The graphs of the presented numerical solutions and analytical solutions at $t = 0(0.2)1$, the graph of the absolute error at $t = 1$ have been plotted in Figure 2 for $h = 1/64$, $\Delta t = 0.05h$ and $P_e = 20000$. From the figure, the approximate solutions were found to be consistent with analytical solutions, and the absolute error at $t = 1$ was observed to be quite small. Then, the absolute errors were calculated for $h = 1/60$, $\Delta t = 0.001$, $\mu = 1.0, 0.1, 0.01$ at $t = 1$ and they were compared with Mittal and Rohila (2020) in Table 4. It can be seen from Table 4 that the absolute errors obtained using these parameters yield results that are virtually identical to those from the Mittal and Rohila (2020) experiments.

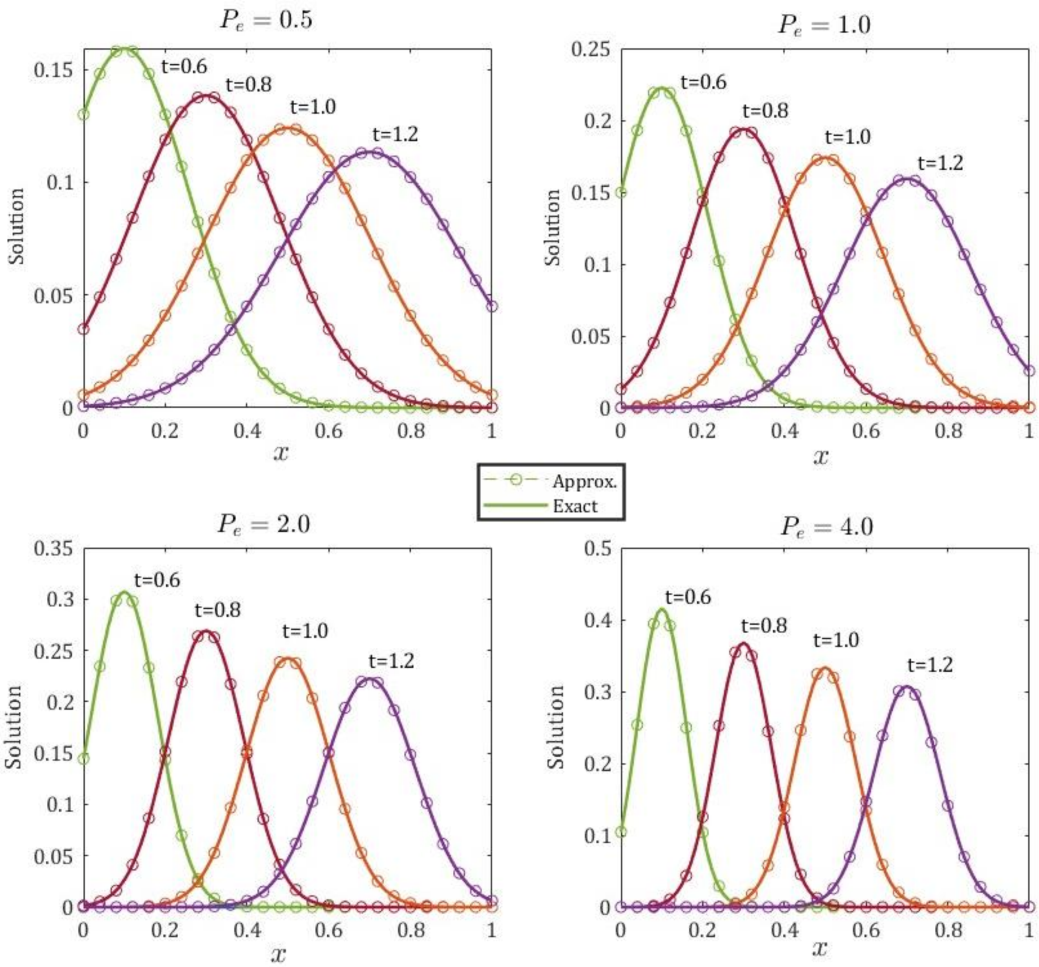

Figure 1. The graphics of numerical (o) and exact (-) solution of Problem 1 for $P_e = 0.5, 1.0, 2.0, 4.0$: $h = 0.01, \Delta t = 0.001$

Table 3. A comparison of absolute errors of Problem 2 for $P_e = 1000, 10000, 20000$ at $t = 1.0$: $h = 1/64$, $\Delta t = 0.05h$

x	Present	Mohebbi and Dehghan (2010)	Mittal and Rohila (2020)	Present	Mohebbi and Dehghan (2010)	Mittal and Rohila (2020)	Present	Mohebbi and Dehghan (2010)	Mittal and Rohila (2020)
	$P_e = 1000$			$P_e = 10000$			$P_e = 20000$		
0.25	9.11e-09	1.43e-06	1.53e-08	8.36e-09	1.06e-06	1.49e-08	8.90e-09	1.02e-04	1.42e-08
0.50	2.22e-08	1.75e-06	3.67e-08	2.21e-08	4.91e-07	3.60e-08	2.34e-08	2.20e-04	3.53e-08
0.75	3.69e-08	1.90e-06	6.08e-08	3.75e-08	6.94e-06	6.32e-08	3.89e-08	3.47e-04	6.51e-08
1.00	4.99e-08	9.75e-07	8.22e-08	5.06e-08	2.56e-05	7.80e-08	5.06e-08	4.71e-04	7.50e-08
1.25	4.93e-08	1.10e-07	8.12e-08	4.93e-08	7.03e-05	9.11e-08	4.92e-08	6.52e-04	9.52e-08
1.50	4.47e-08	2.05e-07	7.32e-08	4.46e-08	1.58e-04	5.60e-08	4.46e-08	8.02e-04	1.16e-08
1.75	3.73e-08	2.88e-07	6.63e-08	3.71e-08	2.69e-04	9.05e-08	3.71e-08	7.40e-04	9.37e-08

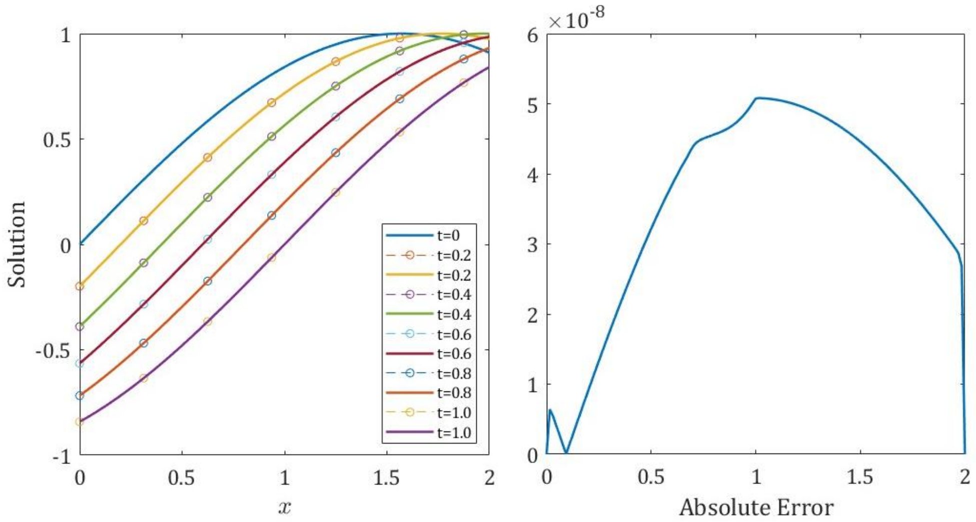

Figure 2. Left: The graphics of numerical solution (o) and exact solution(-), right: The graphic of absolute error at $t = 1$ of Problem 2 for $P_e = 20000$: $h = 1/64$, $\Delta t = 0.05h$.

Problem 3: In this problem, the analytical solution with $\mu = 0.1, \alpha = 1.0$ is given by (Chawla et al., 2000; Mittal and Rohila, 2020; Mohebbi and Dehghan, 2010) as;

$$U(x,t) = e^{5x-\frac{5t}{2}-\frac{\pi^2 t}{40}}\left(\cos\left(\frac{\pi x}{2}\right) + \frac{1}{4}\sin\left(\frac{\pi x}{2}\right)\right),$$

$$x \in [0,1], t \in [0,5]. \tag{30}$$

The absolute errors obtained by the presented method of Problem 3 for $\Delta t = 0.01, 0.001$ and $h = 0.02, 0.01$ at $t = 5$ are presented in Table 5. The Table 5 indicates that the absolute errors are quite small. Next, Table 6 is presented a comparison of the absolute errors obtained for Problem 3 using the presented method with the absolute errors obtained from other studies in the literature for $\Delta t = 0.01$ and $h = 0.01$ at t = 2. It is seen from the table, that the absolute errors of the proposed method are smaller. For $h = 0.01$, $\Delta t = 0.001$, the three-dimensional graph of the numerical solution of Problem 3 in the solution domain $(x,t) \in [0,1]\mathrm{x}[0,5]$, and the graph of the absolute error at t = 5 are presented in Figure 3. As time progressed, a decrease in advection propagation was observed in the graph, and the absolute error was very close to zero at the final time.

Table 4. A comparison of absolute errors of Problem 2 for $\mu = 1.0, 0.1, 0.01$at $= 1 : h = 1/60, \Delta t = 0.001$

x	Present	Mittal and Rohila (2020)	Present	Mittal and Rohila (2020)	Present	Mittal and Rohila (2020)
	$\mu = 1.0$		$\mu = 0.1$		$\mu = 0.01$	
0.1	4.63e-09	4.58e-09	3.90e-09	4.00e-09	4.98e-09	5.59e-09
0.2	8.80e-09	8.74e-09	9.02e-09	9.15e-09	1.13e-08	1.14e-09
0.3	1.25e-08	1.24e-08	1.51e-08	1.52e-08	1.87e-08	1.89e-08
0.4	1.56e-08	1.56e-08	2.19e-08	2.21e-08	2.70e-08	2.72e-08
0.5	1.82e-08	1.81e-08	2.92e-08	2.94e-08	3.60e-08	3.62e-08
0.6	2.02e-08	2.01e-08	3.66e-08	3.68e-08	4.54e-08	4.56e-08
0.7	2.16e-08	2.16e-08	4.39e-08	4.42e-08	5.49e-08	5.52e-08
0.8	2.25e-08	2.24e-08	5.09e-08	5.12e-08	6.41e-08	6.45e-08
0.9	2.28e-08	2.27e-08	5.72e-08	5.75e-08	7.22e-08	7.25e-08

Table 5. The absolute errors of Problem 3 at $= 5$: $\Delta t = 0.01, 0.001$ and $h = 0.02, 0.01$

	$\Delta t = 0.01$		$\Delta t = 0.001$	
x	$h = 0.02$	$h = 0.01$	$h = 0.02$	$h = 0.01$
0.1	1.592116e-10	1.593328e-10	1.461626e-12	1.585555e-12
0.2	4.671363e-10	4.672292e-10	4.531048e-12	4.664998e-12
0.3	1.003891e-09	1.003862e-09	9.936575e-12	1.003584e-11
0.4	1.864114e-09	1.863768e-09	1.868911e-11	1.864813e-11
0.5	3.130599e-09	3.129549e-09	3.174011e-11	3.133653e-11
0.6	4.807195e-09	4.804715e-09	4.935498e-11	4.815146e-11
0.7	6.673586e-09	6.668365e-09	6.973385e-11	6.691043e-11
0.8	7.999574e-09	7.989307e-09	8.627134e-11	8.034616e-11
0.9	7.019997e-09	7.001022e-09	8.248459e-11	7.086434e-11

Table 6. A comparison of absolute errors of Problem 3 at $t = 2$: $\Delta t = 0.01, h = 0.01$

x	Present	Mittal and Rohila (2020)	Rohila (2024)	Mittal and Jain (2012)	Mohammadi (2013)
0.1	4.98e-07	4.99e-07	5.03e-07	5.60e-07	5.02e-07
0.2	1.44e-06	1.44e-06	1.46e-06	1.32e-06	1.16e-06
0.3	3.06e-06	3.06e-06	3.09e-06	2.13e-06	1.81e-06
0.4	5.62e-06	5.62e-06	5.69e-06	2.06e-06	2.06e-06
0.5	9.35e-06	9.36e-06	9.50e-06	1.15e-06	1.15e-06
0.6	1.43e-05	1.43e-05	1.45e-05	7.94e-07	7.94e-07
0.7	1.98e-05	1.98e-05	2.01e-05	6.19e-06	6.19e-06
0.8	2.37e-05	2.37e-05	2.42e-05	1.48e-05	1.48e-05
0.9	2.09e-05	2.08e-05	2.13e-05	1.95e-05	1.95e-05

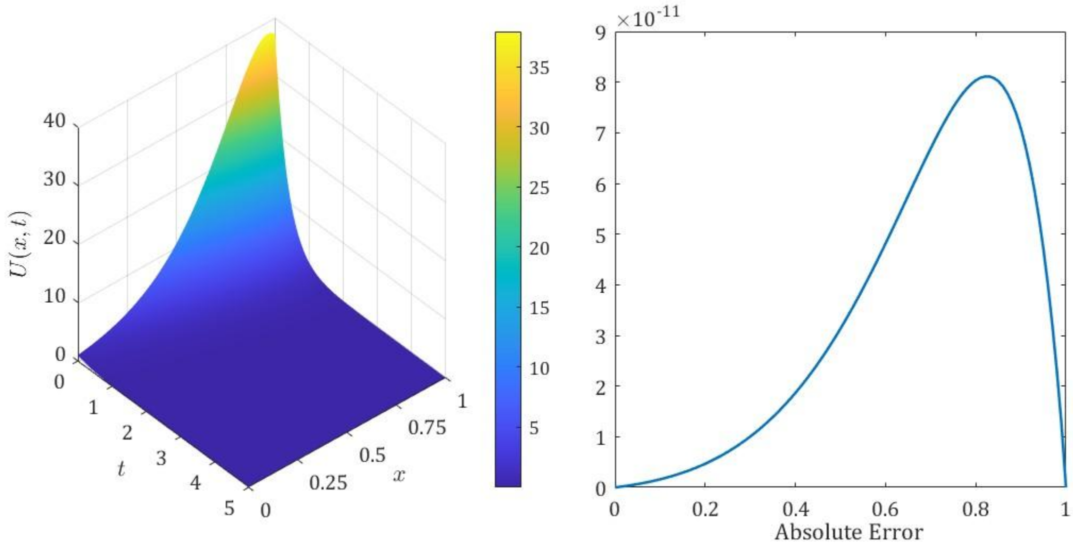

Figure 3. The graph of the numerical solution of Problem 3 in the solution domain $(x, t) \in [0,1]x[0,5]$ for $\mu = 0.1$ and the graph of absolute error at $t = 5$: $h = 0.01$, $\Delta t = 0.001$.

Problem 4: In this problem, the proposed method was tested using the analytical solution of the AD equation in the form given by Mittal and Jain (2012).

$$U(x,t) = \sqrt{\frac{20}{20+t}} \exp\left(-\frac{(x-2-\alpha t)^2}{4\mu(t+20)}\right),$$
$$x \in [0,1], t \in [0,T]. \quad (31)$$

In this problem, it is taken as $\alpha = 0.8$ and $\mu = 0.1$. The approximate solutions and the absolute errors for Problem 4 were calculated at $t = 1.0, 5.0$ for $h = 0.05$ and $\Delta t = 0.01$. The obtained values are shown in Table 7. It can be seen from the table that the numerical solutions of this problem are in good agreement with exact solution and the absolute errors are very small, at levels closer to zero. Subsequently, the absolute errors at different times for $h = 0.01$ and $\Delta t = 0.001$ were calculated, compared with the results in (Mittal and Jain, 2012; Mohammadi, 2013; Nazir et al., 2016) and presented to the readers in Table 8. As shown in the table, the results obtained by the proposed method are better than those from the compared studies. The graphs of the analytical and the approximate solutions for $h = 0.01$, $\Delta t = 0.001$ at times $t = 1.0, 2.0, 3.0, 4.0, 5.0$ are shown in Figure 4. The graph of the absolute error at the final time is also shown in the same graph. The graph shows that the analytical and approximate solutions are in quite strong conformity. A comparison the error norms obtained by the presented method of Problem 4 for $\Delta t = 0.001$, $h = 0.01$ at $t = 1.0, 5.0$ are presented in Table 9. It is seen from the Table 9, that the error norms of the proposed method are smaller at $t = 5.0$.

Table 7. A comparison of approximate and exact solutions of Problem 4 at $t = 1.0, 5.0$: $h = 0.05, \Delta t = 0.01$

	t=1.0			t=5.0		
x	Present	Exact	Absolute Error	Present	Exact	Absolute Error
0.1	0.4097319044	0.4097319360	3.16e-08	0.0275274449	0.0275274321	1.28e-08
0.2	0.4364170366	0.4364171091	7.25e-08	0.0309441357	0.0309441089	2.68e-08
0.3	0.4637346798	0.4637348002	1.20e-07	0.0347154038	0.0347153621	4.17e-08
0.4	0.4915904304	0.4915906039	1.74e-07	0.0388684747	0.0388684175	5.72e-08
0.5	0.5198801437	0.5198803723	2.29e-07	0.0434314357	0.0434313632	7.25e-08
0.6	0.5484903690	0.5484906493	2.80e-07	0.0484331019	0.0484330155	8.64e-08
0.7	0.5772989232	0.5772992421	3.19e-07	0.0539028581	0.0539027621	9.60e-08
0.8	0.6061756046	0.6061759283	3.24e-07	0.0598704765	0.0598703808	9.56e-08
0.9	0.6349830414	0.6349832915	2.50e-07	0.0663659088	0.0663658361	7.27e-08

Table 8. A comparison of absolute errors of Problem 4 at $t = 1.0, 2.0, 5.0$: $h = 0.01, \Delta t = 0.001$

	t=1.0				t=2.0				t=5.0		
x	Present	Nazir et al. (2016)	Mohammadi (2013)	Mittal and Jain (2012)	Present	Nazir et al. (2016)	Mohammadi (2013)	Mittal and Jain (2012)	Present	Nazir et al. (2016)	Mohammadi (2013)
0.1	3.23e-10	2.44e-08	8.71e-09	9 .96e-09	1.53e-12	3.50e-09	7 .71e-09	8 .45e-09	1.29e-10	8.77e-10	1 .73e-09
0.2	7.32e-10	4.00e-08	1 .08e-08	1 .91e-08	6.60e-11	6.15e-09	1 .08e-08	1 .76e-08	2.69e-10	1.45e-09	1 .02e-09
0.3	1.21e-09	4.57e-08	2 .05e-08	2 .70e-08	2.05e-10	7.57e-09	3 .05e-08	2 .71e-08	4.18e-10	1.68e-09	3 .91e-10
0.4	1.74e-09	4.14e-08	3 .60e-08	3 .33e-08	4.15e-10	7.40e-09	3 .60e-08	3 .67e-08	5.72e-10	1.54e-09	1 .96e-09
0.5	2.29e-09	2.73e-08	3 .71e-08	3 .78e-08	6.85e-10	5.46e-09	4 .71e-08	4 .59e-08	7.25e-10	1.02e-09	3 .59e-09
0.6	2.81e-09	5.32e-08	3 .90e-08	4 .02e-08	9.87e-10	1.86e-09	4 .40e-08	5 .38e-08	8.64e-10	1.98e-10	5 .25e-09
0.7	3.19e-09	2.04e-08	3 .74e-08	3 .99e-08	1.26e-09	2.71e-09	3 .74e-08	5 .89e-08	9.60e-10	7.68e-10	6 .94e-09
0.8	3.24e-09	4.17e-08	2 .80e-08	3 .60e-08	1.39e-09	6.71e-09	2 .80e-08	5 .79e-08	9.56e-10	1.54e-09	8 .57e-09
0.9	2.50e-09	4.34e-08	1 .65e-08	2 .55e-08	1.12e-09	7.24e-09	1 .65e-08	4 .36e-08	7.27e-10	1.56e-09	9 .13e-09

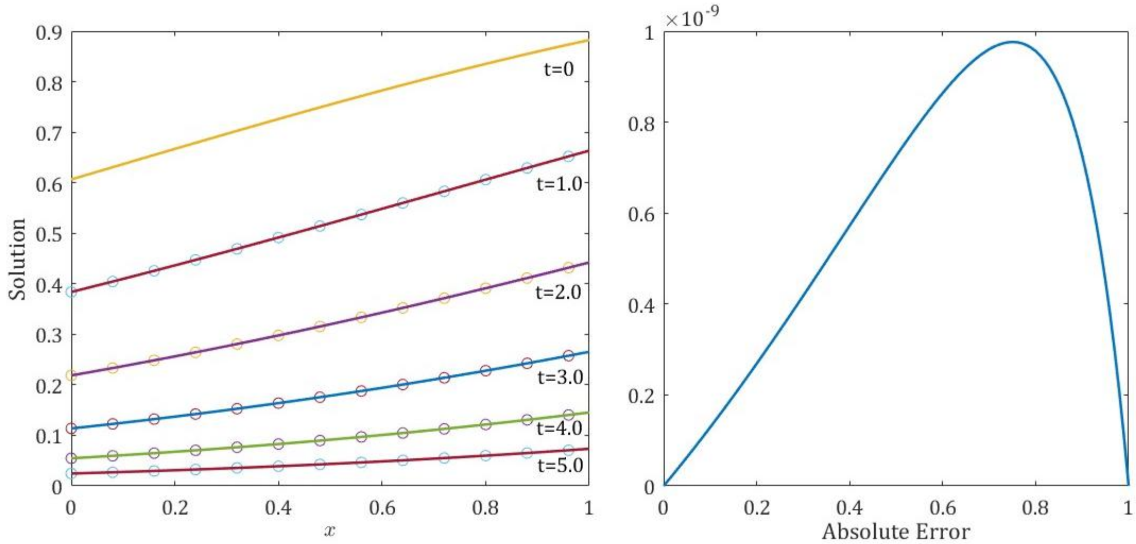

Figure 4. Left: The graphics of numerical solution (o) and exact solution (-) of Problem 4, Right: The graphic absolute error at $= 5$: $h = 0.01, \Delta t = 0.001$.

Table 9. A comparison of error norms of Problem 4 at $t = 1.0, 5.0$: $h = 0.01, \Delta t = 0.001$

	$t = 1.0$				$t = 5.0$			
x	Present		Nazir et al. (2016)		Present		Nazir et al. (2016)	
	L_2	L_∞	L_2	L_∞	L_2	L_∞	L_2	L_∞
0.1	3.23e-10	2.44e-08	8.71e-09	9 .96e-09	1.53e-12	3.50e-09	7 .71e-09	8 .45e-09
0.2	7.32e-10	4.00e-08	1 .08e-08	1 .91e-08	6.60e-11	6.15e-09	1 .08e-08	1 .76e-08
0.3	1.21e-09	4.57e-08	2 .05e-08	2 .70e-08	2.05e-10	7.57e-09	3 .05e-08	2 .71e-08
0.4	1.74e-09	4.14e-08	3 .60e-08	3 .33e-08	4.15e-10	7.40e-09	3 .60e-08	3 .67e-08
0.5	2.29e-09	2.73e-08	3 .71e-08	3 .78e-08	6.85e-10	5.46e-09	4 .71e-08	4 .59e-08
0.6	2.81e-09	5.32e-08	3 .90e-08	4 .02e-08	9.87e-10	1.86e-09	4 .40e-08	5 .38e-08
0.7	3.19e-09	2.04e-08	3 .74e-08	3 .99e-08	1.26e-09	2.71e-09	3 .74e-08	5 .89e-08
0.8	3.24e-09	4.17e-08	2 .80e-08	3 .60e-08	1.39e-09	6.71e-09	2 .80e-08	5 .79e-08
0.9	2.50e-09	4.34e-08	1 .65e-08	2 .55e-08	1.12e-09	7.24e-09	1 .65e-08	4 .36e-08

4. Discussion and Conclusion

In this study, an approximate solution of the one-dimensional linear advection-diffusion equation was obtained using the cubic Hermite B-spline Galerkin method. The main contribution of this paper is the development and validation of an effective numerical method for solving partial differential equations. The proposed method has been shown to be accurate and reliable through its compatibility with analytical solutions and existing studies in the literature, while also providing better results than some previously reported methods. It should also be noted that this is clearly evident when examining the graphs plotted for each model problem, provided that the method is consistent with the physical behavior of the problems. We believe that the method, which performs well in solutions of the advection-diffusion equation without nonlinear terms, may also be effective in numerical solutions of nonlinear partial differential equations. Many computational and applied sciences could benefit from the proposed method, which is expected to facilitate the approximate solution of partial differential equations with distinctive characteristics encountered in the mathematical modeling of various real-world problems.

Author Contributions

The percentages of the authors' contributions are presented below. The authors reviewed and approved the final version of the manuscript.

	H.B.	S.Ö.	Y.U.
C	40	30	30
D	40	30	30
S	20	50	30
DCP	50	30	20
DAI	50	30	20
L	50	30	20
W	40	40	20
CR	40	30	30
SR	40	40	20

C= concept, D= design, S= supervision, DCP= data collection and/or processing, DAI= data analysis and/or interpretation, L= literature search, W= writing, CR= critical review, SR= submission and revision.

Conflict of Interest

The authors declared that there is no conflict of interest.

Ethical Consideration

Ethics committee approval was not required for this study because of there was no study on animals or humans.

References

Başhan, A., Uçar, Y., Yağmurlu, N.M & Esen, A. (2018). A new perspective for quintic B-spline based Crank-Nicolson-differential quadrature method algorithm for numerical solutions of the nonlinear Schrödinger equation. *The European Physical Journal Plus*, 133(1), 12.

Başhan, A., Uçar, Y., Yağmurlu, N.M & Esen, A. (2020). Finite difference method combined with differential quadrature method for numerical computation of the modified equal width wave equation. *Numerical Methods for Partial Differential Equations*, 37, 690–706.

Cecchi, M. M., & Pirozzi, M. A. (2005). High order finite difference numerical methods for time-dependent convection-dominated problems. *Applied Numerical Mathematics*, *55*(3), 334–356.

Chapman, S. J., Shipley, R. J., & Jawad, R. (2008). Multiscale modeling of fluid transport in tumors. *Bulletin of Mathematical Biology*, *70*(8), 2334–2357.

Chatwin P. C., & Allen, C. M. (1985). Mathematical models of dispersion in rivers and estuaries. *Annual Review of Fluid Mechanics*, *17*(1), 119–149.

Chawla, M. M., Al-Zanaidi, M. A., & Al-Aslab, M. G. (2000). Extended one-step time-integration schemes for convection-diffusion equations. *Computers & Mathematics with Applications*, *39*(3–4), 71–84.

Dağ, İ., Canivar, A., & Şahin, A. (2011). Taylor-Galerkin method for advection-diffusion equation. *Kybernetes*, *40*(5–6), 762–777.

Dehghan, M. (2004). Weighted finite difference techniques for the one-dimensional advection–diffusion equation. *Applied Mathematics and Computation*, *147*(2), 307–319.

Ganaie I. A., & Kukreja, V. K. (2014). Numerical solution of Burgers' equation by cubic Hermite collocation method. *Applied Mathematics and Computation*, *237*, 571–581.

Goh, J., Majid, M. A., & Ismail, A. I. M. (2012). Cubic B-spline collocation method for one-dimensional heat and advection-diffusion equations. *Journal of Applied Mathematics*, *2012*.

Guvanasen V., & Volker, R. E. (1983). Numerical solutions for solute transport in unconfined aquifers. *International Journal for Numerical Methods in Fluids*, *3*(2), 103–123.

Iqbal, A., Akram, T., Khan, W. A., & Ali, A. (2023). A Powerful High-Order B-Spline Galerkin Technique for Numerical Solutions of Advection-Diffusion Equation. *International Conference on Soft Computing: Theories and Applications*, 59–68.

Isenberg J., & Gutfinger, C. (1973). Heat transfer to a draining film. *International Journal of Heat and Mass Transfer*, *16*(2), 505–512.

Kadalbajoo M. K., & Arora, P. (2010). Taylor-Galerkin B-spline finite element method for the one-dimensional advection-diffusion equation. *Numerical Methods for Partial Differential Equations*, *26*(5), 1206–1223.

Karahan, H. (2007). Unconditional stable explicit finite difference technique for the advection-diffusion equation using spreadsheets. *Advances in Engineering Software*, *38*(2), 80–86.

Korkmaz, A., & Dağ, I. (2016). Quartic and quintic B-spline methods for advection–diffusion equation. *Applied Mathematics and Computation*, *274*, 208–219. https://doi.org/10.1016/J.AMC.2015.11.004

Mittal, A. K., Ganaie, I. A., Kukreja, V. K., Parumasur, N., & Singh, P. (2013). Solution of diffusion-dispersion models using a computationally efficient technique of orthogonal collocation on finite elements with cubic Hermite as basis. *Computers and Chemical Engineering*, *58*, 203–210.

Mittal, R. C., & Jain, R. K. (2012). Redefined cubic B-splines collocation method for solving convection–diffusion equations. *Applied Mathematical Modelling*, *36*(11), 5555–5573.

Mittal, R. C., & Rohila, R. (2020). The numerical study of advection–diffusion equations by the fourth-order cubic B-spline collocation method. *Mathematical Sciences*, *14*(4), 409–423.

Mohammadi, R. (2013). Exponential B-spline solution of convection-diffusion equations. *Applied Mathematics*, *4*(6), 933–944.

Mohebbi A., & Dehghan, M. (2010). High-order compact solution of the one-dimensional heat and advection-diffusion equations. *Applied Mathematical Modelling*, *34*(10), 3071–3084.

Naghipoor, J., Jafary, N., & Rabczuk, T. (2018). Mathematical and computational modeling of drug release from an ocular iontophoretic drug delivery device. *International Journal of Heat and Mass Transfer*, *123*, 1035–1049.

Nazir, T., Abbas, M., Ismail, A. I. M., Majid, A. A., & Rashid, A. (2016). The numerical solution of advection-diffusion problems using new cubic trigonometric B-splines approach. *Applied Mathematical Modelling*.

Novikau, I., & Joseph, I. (2025). Quantum algorithm for the advection-diffusion equation and the Koopman-von Neumann approach to nonlinear dynamical systems. *Computer Physics Communications*, *309*, 109498.

Palitta, D., & Simoncini, V. (2016). Matrix-equation-based strategies for convection–diffusion equations. *BIT Numerical Mathematics*, *56*(2), 751–776.

Parlange, J. Y. (1980). Water transport in soils. *Annual Review of Fluid Mechanics*, *12*, 77–102.

Prenter, P. M. (1989). *Splines and variational methods*. Wiley.

Rizwan-Uddin. (1997). A second-order space and time nodal method for the one-dimensional convection-diffusion equation. *Computers & Fluids*, *26*(3), 233–247.

Rohila, R. (2024). Numerical Solution of Advection-Diffusion Equation by a Modified Cubic B-Spline Collocation Method. In *Tuijin Jishu/Journal of Propulsion Technology*, *45*(3), 4297 – 4313.

Salkuyeh, D. K. (2006). On the finite difference approximation to the convection-diffusion equation. *Applied Mathematics and Computation*, *179*(1), 79–86.

Ünal, O. (2022). A Stable and High Accurate Numerical Simulator for Convection-Diffusion Equation. *Journal of Advanced Research in Natural and Applied Sciences*, *8*(1), 45–53.

Zlatev, Z., Berkowicz, R., & Prahm, L. P. (1984). Implementation of a variable stepsize variable formula method in the time-integration part of a code for treatment of long-range transport of air pollutants. *Journal of Computational Physics*, *55*(2), 278–301.